

**Atomic structure, adsorbate ordering, and mode of growth of the K/Si(100) $2 \times 1$  surface**

P. Soukiassian\*

*Commissariat à l'Energie Atomique, Service de Recherche sur les Surfaces et l'Irradiation de la Matière,  
Bâtiment 462, Centre d'Etudes de Saclay, 91191 Gif sur Yvette CEDEX, France  
and Département de Physique Université de Paris-Sud, 91405 Orsay CEDEX, France*

J. A. Kubby

*Xerox Webster Research Center, Webster, New York 14580*

P. Mangat and Z. Hurych

*Department of Physics, Northern Illinois University, DeKalb, Illinois 60115-2854*

K. M. Schirm

*Commissariat à l'Energie Atomique, Service de Recherche sur les Surfaces et l'Irradiation de la Matière,  
Bâtiment 462, Centre d'Etudes de Saclay, 91191 Gif sur Yvette CEDEX, France  
and Département de Physique, Université de Paris-Sud, 91405 Orsay CEDEX, France*

(Received 30 April 1992)

We present an investigation of the structural properties, atomic structure, adsorbate mode of growth, and interface formation of the room-temperature K/Si(100) $2 \times 1$  system by a combination of core-level and valence-band photoemission spectroscopies using synchrotron-radiation and scanning-tunneling-microscopy experiments. The results indicate that, at saturation coverage, the potassium atoms appear to form one-dimensional chains parallel to the silicon dimer rows along the  $\langle 110 \rangle$  direction 7.68 Å apart with a single site of adsorption. These K chains pass over the surface step edges to be connected between themselves. The growth and occurrence of a second layer are clearly related to the presence of impurities which, even at very low levels, are shown to significantly increase the K sticking coefficient. It demonstrates the extreme sensitivity of this system and stresses the crucial importance of quality in surface preparation and alkali-metal deposition. At a lower coverage, the K atoms are adsorbed on various coexisting sites with no long-range order. An ordering transition leading to the formation of the one-dimensional linear K metallic chains occurs. The adsorbate-adsorbate interaction is the dominant driving force in this adsorbate-ordering transition. The valence-band results indicate that the K atoms are covalently bonded to the Si atoms through the dangling bond, which makes the cave the most favorable adsorption site for the K atoms. This investigation brings new insights into the understanding of the structural properties of (alkali metal)/Si(100) $2 \times 1$  systems.

**I. INTRODUCTION**

The electronic and structural properties of alkali-metal adsorption on the Si(100) $2 \times 1$  surface have been intensively investigated in recent years by use of various experimental techniques or theoretical methods.<sup>1-26</sup> In contrast to most of the recent experimental investigations of the electronic properties which were performed with the use of rather sophisticated techniques, the atomic structure of this system was, until recently, mainly studied by conventional electron-diffraction techniques. A structural model was proposed nearly two decades ago by Levine on the basis of traditional low-energy electron-diffraction (LEED) measurements for the Cs/Si(100) $2 \times 1$  system.<sup>9</sup> He suggested that Cs atoms form one-dimensional alkali-metal chains (ODAC) with a single site of adsorption, the pedestal site (see Fig. 1). Like Cs,<sup>9</sup> K on Si(100) $2 \times 1$  was found to exhibit the same  $2 \times 1$  LEED pattern at all coverages.<sup>10</sup> Therefore, the same ODAC model was suggested to be also suitable for the K/Si(100) $2 \times 1$  surface.<sup>10</sup> This model was later supported

by other experimental investigations using electron-energy-loss spectroscopy or dynamical LEED techniques<sup>4,12</sup> and theoretical calculations.<sup>5</sup> It is only recently that several experimental works using photoelectron diffraction with single scattering analysis,<sup>17</sup> medium energy-ion scattering,<sup>20</sup> dynamical LEED,<sup>21</sup> reflection high-energy electron diffraction measurements,<sup>22</sup> and photoemission adsorbed xenon<sup>23</sup> suggested that, on the Si(100) $2 \times 1$  surface, the alkali-metal atoms form two layers with two sites of adsorption. Three theoretical investigations using a pseudopotential have also favored such double-layer models<sup>24-26</sup> In all these studies suggesting double-layer models, various sites of adsorption, depending on the experimental or theoretical technique, were proposed including two of the following pedestal, valley-bridge, or cave sites.<sup>17,20-26</sup> Ling Ye, Freeman, and Delle using a total-energy *ab initio* molecular calculations with a large cluster investigated the stability of each proposed site of adsorption.<sup>8</sup> In contrast to previous results, they have shown that the cave site is a more stable site of adsorption for K atoms on the Si(100) $2 \times 1$  (Ref. 8) than

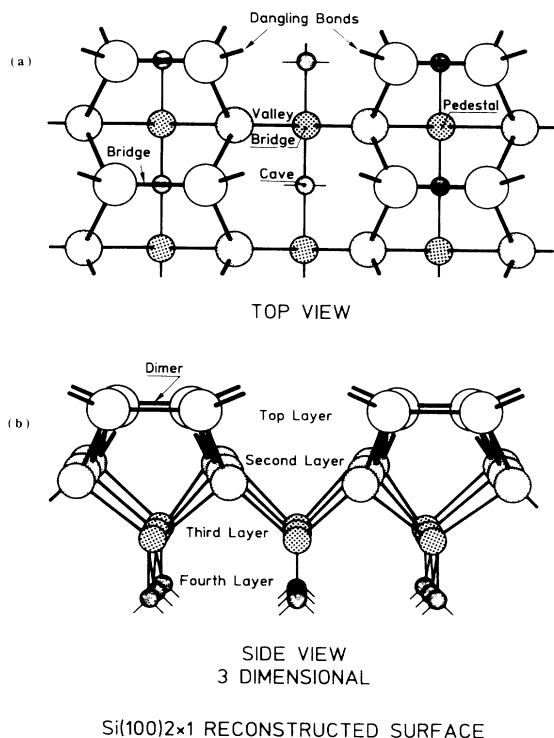


FIG. 1. Top view model of the reconstructed Si(100)2 $\times$ 1 surface showing the various possible adsorption sites for K atoms proposed in the literature. (b) Three-dimensional 3(D) side view model of the reconstructed Si(100)2 $\times$ 1 in the case of symmetric dimers.

the pedestal (Fig. 1) one proposed on the basis of LEED measurements.<sup>10</sup>

In this paper, we report room-temperature scanning tunneling microscopy (STM) and core-level photoemission spectroscopy using synchrotron-radiation investigations of the K/Si(100)2 $\times$ 1 surface in the monolayer range. The topographic images with atomic resolution show that, at one K monolayer (ML), K atoms form one-dimensional metallic chains distant by 7.68 Å along the  $\langle 110 \rangle$  direction and parallel to the Si dimer rows. The adsorbate-adsorbate interaction is found to be stronger than the adsorbate-substrate one. The mode of growth is monitored by core-level photoemission spectroscopy. These results support a model with a single site of adsorption (CAVE) and single chain at saturation coverage. We also clearly demonstrate that the growth and occurrence of a second layer could only be related to the presence of impurities, even at very low levels.<sup>27</sup>

## II. EXPERIMENTAL DETAILS

The photoemission experiments were performed at the Synchrotron Radiation Center of the University of Wisconsin-Madison. The radiation emitted by the Aladdin 1 GeV storage ring was dispersed by 6-m toroidal grating TGM and grasshopper mark II monochromators. The photoelectron energy was analyzed with an angle in-

tegrating double-pass cylindrical mirror analyzer. The overall energy resolution, which was controlled by the use of Au 4*f* core level and Au valence band was found to be better than 0.3 eV. The data were taken in a vacuum chamber at a pressure better than  $4 \times 10^{-11}$  Torr. The STM measurements were performed at the Xerox Webster Research Center in an ultrahigh vacuum chamber equipped with a third generation small-size scanning tunneling microscope using a cylindrical piezoelectric ceramics for scanning.<sup>28</sup> The pressure during data acquisition was  $1.2 \times 10^{-10}$  Torr including mainly a partial pressure of molecular hydrogen ( $8 \times 10^{-11}$  Torr), carbon monoxide ( $1.6 \times 10^{-11}$  Torr), water ( $5.7 \times 10^{-12}$  Torr), and atomic oxygen and methane ( $5.5 \times 10^{-12}$  Torr). The Si(100)2 $\times$ 1 surfaces were prepared in both types of experiments using the same standard by thermal annealings below 900°C at background pressures always in the low  $10^{-10}$  Torr. Alkali metals on surfaces have been shown to enhance the sticking coefficient of inorganic and/or organic molecules,<sup>29</sup> which explain the very high sensitivity of the structural as well as electronic properties of these systems to very small amounts of oxygen or other molecules.<sup>30-32</sup> In fact, the presence of such species on a surface covered with alkali metals could lead in unexpected charge transfer and reduced radii and results in significant misinterpretations. The K overlayers were deposited on the Si(100)2 $\times$ 1 surface by using SAES Getters chromate sources which were very carefully outgassed. In these conditions, the pressure increase during potassium deposition was never above  $1 \times 10^{-11}$  Torr. In fact, these sources, when not outgassed correctly, have been found to release hydrogen, carbon monoxide, and/or oxygen.<sup>33</sup> Finally, the various K depositions were, in all cases, performed on freshly cleaned and renewed Si(100)2 $\times$ 1 surfaces. We label the potassium saturation coverage as 1 monolayer (1 ML), meaning one physical potassium layer, which corresponds to a surface coverage of  $\Theta = 0.5$ , i.e., 1 K atom per Si dimer.<sup>1,6,7,12,13</sup> All other experimental details could be found elsewhere.<sup>7,13,28</sup>

## III. RESULTS

### A. STM results

The STM measurements on an alkali-metal covered surface are not, in general, easy to perform. In fact, alkali-metal adsorption on a surface decreases dramatically the surface work function. Furthermore, we have shown that the bonding between alkali-metal atoms and silicon surfaces is weak and covalent<sup>7</sup> while the bonding with tungsten or other transition metal is also covalent but strong.<sup>34</sup> This means that one has to select working conditions in which the tip does not come too close from the silicon surface in order to avoid presence of alkali-metal atoms on the tip which could dramatically modify the results. Also, since it was shown that alkali-metal-silicon bonding has a dominant covalent character,<sup>7</sup> one can anticipate that the tip would tunnel not only into the alkali-metal atom but also, at least in part, into its bonding to the surface, i.e., into the dangling bond.<sup>27</sup> In order to be able to trace the orientation of possible

alkali-metal chains,<sup>9,10</sup> we have performed the STM measurements on stepped ( $4^\circ$ ) Si(100) $2\times 1$  single domain terraces that are large enough to represent the Si(100) $2\times 1$  surface. The terraces are separated by double-height steps. In this case, the step edges are perpendicular to the silicon dimer rows, i.e., in the  $\langle 110 \rangle$  direction.

In order to trace the presence of K overlayer in the investigated area of the Si(100) $2\times 1$  surface, we have first performed electron interferometry by measuring the conductivity versus the distance between the tip and the surface.<sup>35</sup> The corresponding conductivity standing waves are very sensitive to surface-work-function changes. Figure 2 displays the standing-wave measurements for the clean Si(100) $2\times 1$  and the 1 ML K/Si(100) $2\times 1$  surfaces performed as described elsewhere for other systems.<sup>35</sup> As can be seen from Fig. 2, the first maximum and the other peaks are shifted by nearly 1.8 eV upon K deposition. This behavior results from the dramatic decrease of the local surface work function  $\Delta W$  upon potassium deposition ( $\Delta W = -3.2$  eV),<sup>36</sup> to which the onset of conductivity standing waves is very sensitive. It confirms that the investigated surface area is covered by potassium.

Figures 3(a) and 3(b) exhibit the topographic images for the (1 ML K)/Si(100) $2\times 1$  system by tunneling into the filled and empty states, respectively (taken in the same scan), with a bias of  $\pm 1.2$  V. As can be seen from Fig. 3(a), the K atoms form one-dimensional linear chains separated by 7.68 Å and parallel to the silicon dimer rows along the  $\langle 110 \rangle$  direction. In this way, the K-covered surface looks very similar to the clean Si(100) $2\times 1$  stepped ( $4^\circ$ ) surface,<sup>28</sup> which is in very good agreement with the  $2\times 1$  pattern diffraction observed by LEED experiments<sup>10</sup> also on the K-covered surface. One should also notice that the K chains are observed in Fig. 3 with a very good contrast. Another aspect that could be clearly seen from Fig. 3 is the fact that these potassium chains are passing over the step edge and are connected to chains located on the next terrace. This feature appears even more clearly in Figs. 4(a), 4(b), and 4(c) which

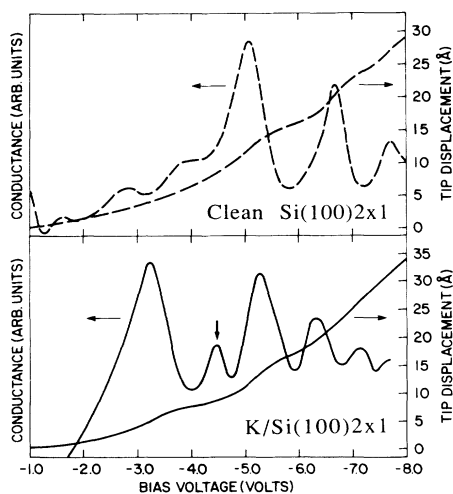


FIG. 2. Conductivity standing-wave measurements for the (a) clean Si(100) $2\times 1$  and (b) 1 ML K/Si(100) $2\times 1$  surfaces.

display the topographic images (height map, height side view, and curvature map, respectively) for the same system in another area of the surface. The steps appear to be rounded which could be an affect of either the K atoms or tip-step convolution giving rise to anomalous images. In fact, when a surface feature has a radius of curvature similar to, or smaller than the tip, the sharp surface feature can image the tip, thus convoluting the image. Also, it is interesting to note that the topographic images given by tunneling into the filled and empty states [Figs. 3(a) and 3(b)] are superimposed without the phase shift seen on the clean surface, which indicates that these chains are metallic as previously shown for the K/Si(100) $2\times 1$  surface by other experimental or theoretical investigations.<sup>4,5</sup> Also of interest in Fig. 3 is the presence of two small three-dimensional potassium clusters

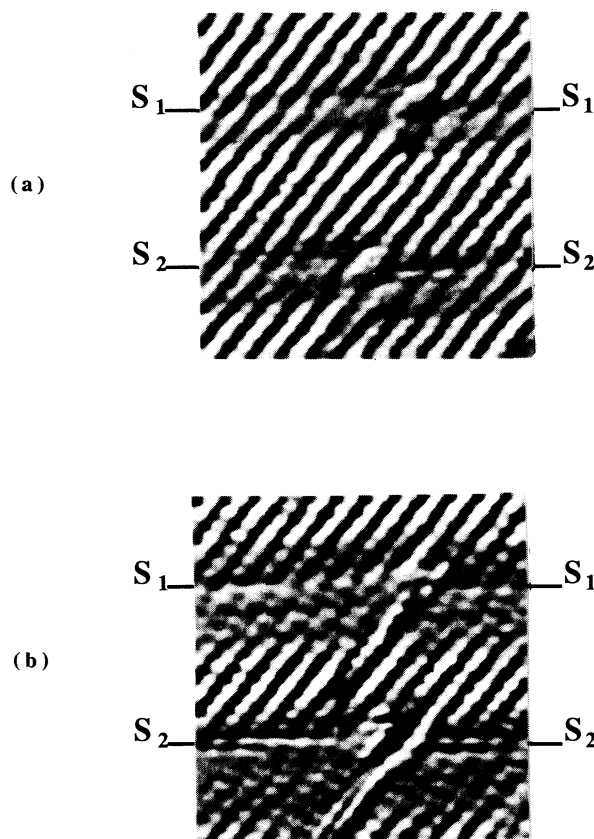


FIG. 3. Curvature STM image (filled states) of 1 ML of potassium on the Si(100) $2\times 1$  ( $4^\circ$ )-stepped surface. The tip bias was  $V_t = +1.2$  V and the tunneling current was 1 nA. The two steps are noted as  $S_1$  and  $S_2$ . The potassium chains are formed along the  $\langle 110 \rangle$  direction and the distance between two chains is 7.68 Å. Notice the two 3D potassium clusters on the step edges. The image has not been corrected for drift. The maximum pressure rise  $\Delta P$  during potassium deposition remained below  $1\times 10^{-11}$  Torr. (b) Curvature STM image (empty states) of 1 ML of potassium on the Si(100) $2\times 1$  ( $4^\circ$ )-stepped surface. The tip bias was  $V_t = -1.2$  V and the tunneling current was 1 nA. The maximum pressure rise  $\Delta P$  during potassium deposition remained below  $1\times 10^{-11}$  Torr.

on the step edges. In the present STM experiments, the measured corrugations were 1.5 and 0.7 Å by tunneling, respectively, into the filled and empty states. Using the K-Si bond length of 3.14 Å measured by surface-extended x-ray-absorption fine structure (SEXAFS),<sup>6</sup> one can determine the largest geometrical height difference between a “top” chain (pedestal) and a “valley” chain (cave or valley bridge). This gives height differences of 0.54 Å between the pedestal and cave sites and 1.04 Å between pedestal and valley-bridge sites. However, it is rather difficult to compare directly these values with the above-measured corrugations which are more distances between electronic states, since there is no available calculation providing the density-of-charge contours of the K atom

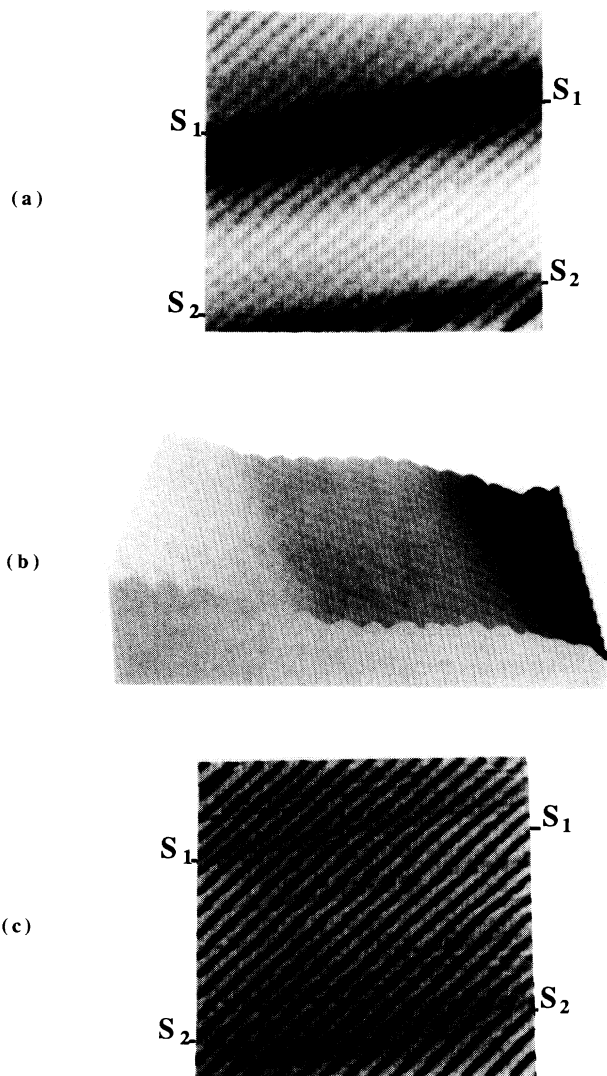


FIG. 4. (a) Height STM image (filled states) of 1 ML of potassium on the Si(100)2×1 for another area. The two steps are noted as S<sub>1</sub> and S<sub>2</sub>. The image has not been corrected for drift. The tip bias was  $V_t = +1.2$  V and the tunneling current was 1 nA. The maximum pressure rise  $\partial P$  during potassium deposition remained below  $1 \times 10^{-11}$  Torr. (b) 3D side view of (a). (c) Curvature map of (a). The two steps are noted as S<sub>1</sub> and S<sub>2</sub>.

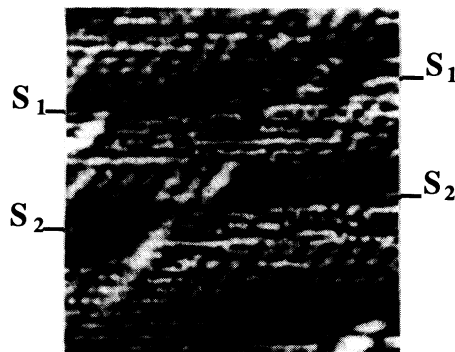


FIG. 5. Curvature STM image (filled states) of 0.4 ML of potassium on the Si(100)2×1-4°-stepped surface. The tip bias was  $V_t = +1.2$  V and the tunneling current was 1 nA. The two steps are noted as S<sub>1</sub> and S<sub>2</sub>. The image has not been corrected for drift. The maximum pressure rise  $\Delta P$  during potassium deposition remained below  $1 \times 10^{-11}$  Torr.

for the various adsorption sites on the Si(100)2×1 surface. Therefore, it is not possible to clearly determine the K adsorption site only on the basis of these STM measurements.

We now turn to the submonolayer coverage regime by looking at Fig. 5 which displays the topographic STM image of the (0.4 K ML)/Si(100)2×1 (i.e.,  $\Theta = 0.2$ ; the K coverage was estimated from the evaporation time—see the following sections) surface by tunneling into the filled states with a bias of +2.75 V. On this picture, the clean silicon surface appears clearly in various areas of the three terraces that can be seen. Potassium adsorbate atoms are seen to be adsorbed on various coexisting sites including dangling bonds, and pedestal and cave sites (later a K atom is located in the top left part of the picture) with no long-range order. Also, there are some few small chains perpendicular to the  $\langle 110 \rangle$  direction as previously reported for Li/Si(100)2×1.<sup>19</sup> Since the direction of the scans were also parallel to the step edge, one cannot totally rule out the possibility that these chains could result from tip-induced motion of adsorbate atoms. The finding that K atoms are adsorbed on various coexisting sites suggests that the adsorption energies for each of these sites are rather close, which supports the recent results of total-energy calculations finding that there is not too much difference between the adsorption energies for the various investigated adsorption sites.<sup>8,26</sup>

### B. Mode of growth

We have monitored the growth of the potassium overlayer by the use of K 3*p* and Si 2*p* core levels. Figures 6(a) and 6(b) exhibit the K 3*p* and Si 2*p* core levels for various potassium evaporation time. Figure 7(a) displays the integrated intensity dependence of K 3*p* and Si 2*p* core levels versus evaporation time. As can be seen from Figs. 6(a) and 7(a), the intensity of the K 3*p* core level increases until an evaporation time of about 130 sec and then reaches a constant value for longer evaporation time. Similarly, the Si 2*p* core level line displayed in Figs.

6(b) and 7(a) undergoes a linear decrease of its intensity upon potassium deposition up to 130 sec, after which its intensity remains constant. This means that a saturation in the coverage occurs about this time that we assign to the completion of one full physical K monolayer (ML) meaning 1 K atom per silicon dimer with a surface coverage of  $\Theta=0.5$ . This is likely to result from the decrease of the K sticking coefficient at coverages near 1 ML. This behavior is similar to what we have previously observed for other alkali metals (Na, Rb, and Cs) on the same or other silicon surfaces<sup>7,13,29,37</sup> as well as other very different surfaces such as metals.<sup>30,32</sup> It is important to mention here that the pressure increase  $\Delta p$  during these potassium depositions [Figs. 5(a), 5(b), and 6] always remained below  $1 \times 10^{-11}$  Torr. The surface was renewed after each potassium deposition.

In order to investigate the effect of pressure increases during the deposition of alkali metal, we have intentionally performed the same experiment in exactly the same

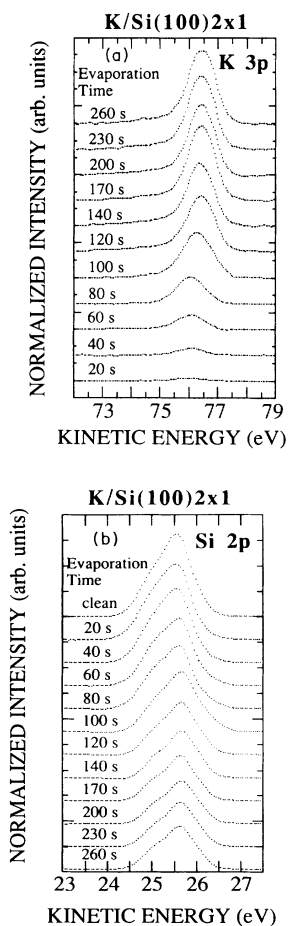


FIG. 6. (a) K 3p core-level photoemission spectra at various potassium evaporation time for the K/Si(100)2 $\times$ 1 system. The photon energy was 100 eV. The maximum pressure rise  $\Delta P$  during potassium deposition remained below  $1 \times 10^{-11}$  Torr. (b) Si 2p core-level photoemission spectra at various potassium evaporation time for the K/Si(100)2 $\times$ 1 system. The photon energy was 130 eV. The maximum pressure rise  $\Delta P$  during potassium deposition remained below  $1 \times 10^{-11}$  Torr.

conditions (meaning the same geometry and the same evaporation current measured accurately by a digital amperemeter) except that the potassium source was only partially outgassed resulting in slightly larger pressure increases during K deposition. The integrated intensity dependence of K 3p and Si 2p core levels versus the time of evaporation are displayed in Fig. 7(b) for a pressure rise remaining below  $1 \times 10^{-10}$  Torr. It is striking to note in Fig. 7(b) that the K 3p core-level intensity does not exhibit saturation and undergoes a linear increase even above the saturation coverage of one monolayer (130 sec) observed above in Fig. 7(a). This behavior indicates that more K atoms can be adsorbed which results in the growth of additional K layers. Figure 7(c) shows the same features for a pressure increase of  $\Delta p \leq 6 \times 10^{-10}$  Torr during K deposition. The K 3p core-level intensity also increases linearly up to 180 sec evaporation time for which there is a clear increase in the slope. It is interesting to remark that the valence-band spectra obtained with a pressure rise of  $1 \times 10^{-10}$  Torr did not exhibit a noticeable trace of contamination, unlike the same valence-band data obtained for a pressure increase of  $6 \times 10^{-10}$  Torr. A gas analysis during alkali-metal deposition indicate that these chromate dispensers (SAES Getters) release hydrogen, oxygen, and carbon monoxide when not very carefully outgassed.<sup>33</sup> Since alkali metals are known to enhance dramatically the sticking coefficient of these species,<sup>29,37</sup> both are likely to be codeposited on the Si(100)2 $\times$ 1 surface under these conditions and result in higher sticking coefficient for K atoms in the presence of acceptor species such as oxygen or carbon monoxide. Furthermore, we have shown by photo-stimulated ion desorption (PSD) (a very sensitive tool to probe the presence of hydrogen atoms and their environment) on alkali-metal-covered Si(100)2 $\times$ 1 surfaces that hydrogen is also bonded to alkali atoms<sup>38</sup> and is likely to form alkali hydrides<sup>39</sup> which could enhance K-K lateral interactions through hydrogen atoms.

### C. Electronic properties

We now discuss the valence-band results. Figure 8 displays the valence-band spectra for the clean Si(100)2 $\times$ 1 surface and covered by various amounts of potassium up to the saturation (1 monolayer, i.e.,  $0 \leq \Theta \leq 0.5$ ). Since these measurements are performed with an angle-integrating analyzer, the spectra which are shown in Fig. 8 reflect the density of states (DOS) of the K/Si(100)2 $\times$ 1 system. The clean Si(100)2 $\times$ 1 surface exhibits several features including, in particular, peaks A and B which are related to Si 3p electronic levels. Peak A, located at  $\approx 1$  eV below the valence-band maximum for the clean surface is an electronic surface state related to the silicon dangling bond. The behavior of peak A is of special interest since it is not destroyed upon K adsorbate deposition as one would normally expect for a surface state.<sup>34</sup> Instead, its intensity increases dramatically upon potassium coverages between 0 and 1 monolayer while it is shifted to higher binding energy by 0.5 eV, in very good agreement with the DOS calculated by Ling Ye, Freeman, and Delley.<sup>8</sup> The increase in the binding energy results from bonding formation between the K ad-

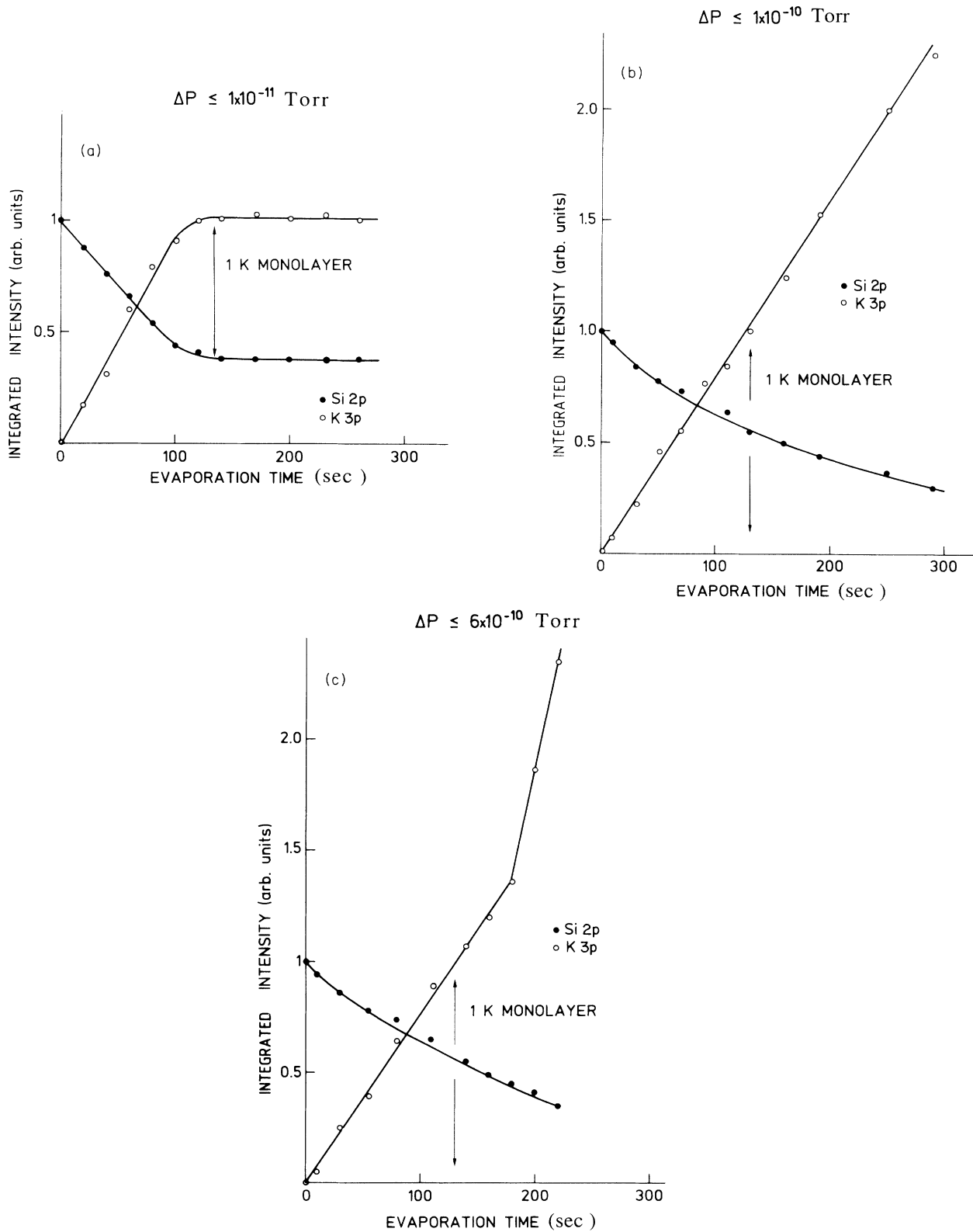


FIG. 7. (a) K 3p and Si 2p integrated intensity vs the potassium evaporation time for the K/Si(100)2×1 system. The maximum pressure rise  $\Delta P$  during potassium deposition remained below  $1 \times 10^{-11}$  Torr. Note that the saturation coverage of 1 K monolayer corresponds to 1 K per Si dimer. (b) K 3p and Si 2p integrated intensity vs the potassium evaporation time for the K/Si(100)2×1 system. The maximum pressure rise  $\Delta P$  during potassium deposition remained below  $1 \times 10^{-10}$  Torr. (c) K 3p and Si 2p integrated intensity vs the potassium evaporation time for the K/Si(100)2×1 system. The maximum pressure rise  $\Delta P$  during potassium deposition remained below  $6 \times 10^{-10}$  Torr.

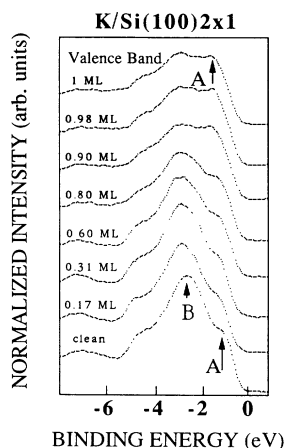


FIG. 8. Valence-band spectra for the K/Si(100)2 $\times$ 1 system at various K coverages between 0 and 1 monolayer. The photon energy was 82 eV. The maximum pressure rise  $\Delta P$  during potassium deposition remained below  $1 \times 10^{-11}$  Torr.

sorbate and the Si substrate similar to the case of other alkali-metal-covered surfaces.<sup>7,34</sup> Since the cross section of the K 4s valence electron is very low at the photon energy used here, i.e., 82 eV, one cannot interpret simply this increase in intensity as a result of the emission of K 4s.<sup>40</sup> Rather, this feature could only be explained if the K 4s valence electron hybridizes with the Si 3p surface state related to the dangling bond. In this case, the nature of the K 4s orbital would somewhat change by hybridization with the Si 3p dangling bond which is localized, explaining why it could be observed here. Therefore, at 1 K ML, peak A indicates the formation of a K 4s–Si 3p electronic interface state involving the silicon dangling bond. Similarly, we have observed the same electronic interface states for other (alkali metal)/Si(100)2 $\times$ 1 or Ge(111)2 $\times$ 1 interfaces.<sup>7,29,31,41</sup> It indicates that the nature of the bonding between K and Si atoms is covalent as we previously reported for Na- or Cs-covered Si(100)2 $\times$ 1 surfaces.<sup>7,29,41</sup> It is also in excellent agreement with the recent metastable deexcitation spectroscopy (MDS) experiments by Nishigaki *et al.* who have demonstrated for the same system that the K 4s valence electron is occupied<sup>14</sup> as well as with high-resolution core-level photoemission spectroscopy investigations for another K-covered silicon surface by Ma *et al.*<sup>42</sup> This covalent bonding is weak since (i) the bond length between K and Si is rather large at 3.14 Å as measured by SEXAFS (Ref. 6) and (ii) the temperature of desorption of K from the Si(100)2 $\times$ 1 surface is rather low (600°C).<sup>6,29</sup> Furthermore, this covalent bonding is also polarized as a result of the important surface-work-function decrease (–3.2 eV) upon K deposition.<sup>36</sup>

#### IV. DISCUSSION

The above results suggest that, at one potassium monolayer (meaning a surface coverage of  $\Theta=0.5$ , i.e., 1 K atom per Si dimer or per 2 Si atoms), K atoms are adsorbed on the Si(100)2 $\times$ 1 surface as one-dimensional chains distant by 7.68 Å and parallel to the Si dimer rows

along the  $\langle 110 \rangle$  direction which also implies a single site of adsorption for the K atoms. Also, the situation at 0.4 K ML ( $\Theta=0.2$ ; see Fig. 5), where K atoms are sitting on various coexisting sites of adsorption indicates that, an ordering transition occurs between low coverages and the saturation coverage of 1 K ML. This drives the formation of the one-dimensional chain observed at 1 K ML in Figs. 3 and 4. It indicates that, as soon as the K-K distance becomes smaller with increasing coverages, the adsorbate-adsorbate interaction becomes stronger than the adsorbate-substrate interaction which is known to be weak.<sup>6,7</sup> The K-K interaction, which has a metallic character, is the leading driving force in this ordering transition. It also demonstrates that the alkali-metal–alkali-metal interaction, which was so far neglected in the theoretical investigations of these systems, has also to be taken into account. Interestingly, the K chains pass over the step edges to be connected to the chains of the next terrace. This further suggests that, at 1 K ML, a K atom prefers to be bonded to another K atom and that the influence of the substrate structure on the adsorbate ordering, while significant enough to drive the chain formation along the  $\langle 110 \rangle$  direction, is weaker than the K-K interaction. It also shows that it is less costly in energy for a K chain on a given terrace to be bonded to the K chain located on the next terrace than to follow the substrate registry at the step edge. Our results are also in agreement with the fact that these one-dimensional chains are metallic as first proposed by Levine for the Cs/Si(100)2 $\times$ 1 system<sup>9</sup> and confirmed more recently by various experimental works using different techniques or theoretical calculations for K/Si(100)2 $\times$ 1 surfaces.<sup>4–6,43</sup>

We have now to comment on the dramatic effects induced by impurities on the mode of growth of the K adsorbate. As shown above in Fig. 7(a) and from the STM images provided in Figs. 3 and 4, when the pressure rise  $\Delta P$  upon K deposition remains below  $1 \times 10^{-11}$  Torr (which is the standard that we have been using commonly in our previous works), the saturation coverage occurs at 1 monolayer which corresponds to 1 K atom per 2 Si atoms ( $\Theta=0.5$ ). This means that, when the saturation coverage is reached at room temperature, the sticking coefficient become negligible. However, when the pressure rise  $\Delta P$  upon K deposition is larger by one order of magnitude at  $1 \times 10^{-10}$  Torr [Fig. 7(b)], it is clear that additional K atoms could be deposited on the surface leading to the growth of a second layer. Because of their exceptional role as catalysts, alkali metals including potassium are known to enhance dramatically the sticking coefficient of inorganic and organic molecules.<sup>29,37</sup> This means that when the SAES Getters chromate sources used here as well as in many other works are not correctly outgassed, the alkali metal is codeposited with various other species which are also released from the SAES Getters dispensers. As described above, it has been shown that, in these conditions, these alkali-metal sources mainly release hydrogen, oxygen, carbon monoxide, and methane.<sup>29,33</sup> The presence of acceptor species such as oxygen or carbon-monoxide molecules could result in charge transfer from the alkali-metal adsorbate to the antibonding orbital of the molecule<sup>29,37,44–46</sup> leading

to a reduced radius for the K atoms which, in itself, is likely to be enough to produce significant structural changes. In this context, it is also interesting to notice that the ordering of an alkali-metal overlayer is very sensitive to a small amount of oxygen.<sup>32</sup> The presence of hydrogen on the surface could also dramatically affect the K adsorption since H atoms are known to bond to the Si dangling bond<sup>47</sup> and could therefore compete with the alkali-metal atoms which are also bonded to the same dangling bonds. The above STM results have shown that the structure of the K atoms results from a very delicate balance between adsorbate-adsorbate versus adsorbate-substrate interactions. Therefore, as soon as the distance between two K atoms becomes smaller with increasing coverage, the K-K interaction becomes stronger than the K-Si interaction (which is known to be weak<sup>6,7</sup>) and appears to be the leading driving force in the formation of the one-dimensional alkali-metal linear chains observed in Figs. 3 and 4. Furthermore, our recent PSD experiments on (alkali metal)/Si(100)2×1 systems have shown that hydrogen is bonded to the alkali atoms<sup>38</sup> to form alkali hydrides.<sup>38,39</sup> In these views, it is then easy to imagine that the presence of impurities, even in very small amounts, could significantly modify the above equilibrium and results in the growth of an additional K overlayer as demonstrated above when the pressure rise  $\Delta P$  is about  $1 \times 10^{-10}$  Torr during K deposition. In that respect, the presence in Fig. 3(a) of two small three-dimensional K clusters near the step edges, which could be interpreted as resulting from higher sticking probability on a surface defect, could also be due to the presence of a small amount of hydrogen in this area holding together several K atoms with formation of K hydrides. It is likely that the very delicate balance between the K-K and K-Si interactions could be disrupted by foreign atoms. It is also possible that the lateral K-K interaction (between 2 K chains) is increased by the presence of impurities leading to the growth of an additional layer as observed in Figs. 7(b) and 7(c). The very high sensitivity to impurities of surfaces covered by alkali metals stresses once again<sup>13,29,40,41</sup> the crucial importance of surface preparation (especially the quality of the alkali-metal layer and the necessity of a very high standard of cleanliness) since it is very likely to be responsible of the many present controversies between various structural models. Our results do not support two-layer models with two different sites of adsorption as favored by some experimental works and/or pseudopotential calculations.<sup>17,20-26,43</sup>

While the STM results demonstrate that K atoms appear to be adsorbed along one-dimensional metallic chains parallel to the  $\langle 110 \rangle$  direction with a single site of adsorption, it was not possible to determine the site of adsorption at saturation coverage from these measurements since the entire surface was covered and due to the lack of available calculation providing charge contours of the K atom for the various adsorption sites on the Si(100)2×1 surface. The valence-band results have shown that the K 4s valence electron hybridizes with the Si 3p dangling bonds, leading to the formation of a covalent bonding. This suggests that the K atoms are bonded to the silicon dangling bonds, in which case the

cave site of adsorption is likely to be the most favorable site for K atoms since each potassium would be bonded to two silicon dangling bonds (see Fig. 1). From this point of view, the situation is less favorable for the other sites, especially for the valley bridge for which the closest Si atoms would not have any dangling bond. Our interpretation is in very good agreement with the recent *ab initio* total-energy molecular DMol calculations.<sup>8</sup> Finally, it is interesting to note that these results are also in excellent agreement with our recent photoemission extended x-ray-absorption fine-structure investigations of the Na/Si(100)2×1 system which shows that Na atoms have also one single adsorption site at the monolayer coverage (1 Na atoms per Si dimer) which is the cave site.<sup>48</sup>

## V. CONCLUSIONS

We have shown that, at saturation coverage (1 K atom per Si dimer), K atoms adsorbed on the Si(100)2×1 surface form one-dimensional linear metallic chains 7.68 Å apart and parallel to the Si dimer rows along the  $\langle 110 \rangle$  direction with a single site of adsorption. The growth of a second layer could only occur in the presence of impurities (even at very low levels). It stresses the crucial importance of the quality of surface preparation and alkali-metal deposition and indicates the extreme sensitivity of alkali-metal-covered surfaces to impurities. On each (100)2×1 terrace, these K chains are passing over the step edges to be connected to the chains presents on the next terrace which indicates that the K-K interaction is stronger than the K-Si interaction. At 0.4 potassium monolayer ( $\Theta=0.2$ ), the K atoms are adsorbed on various coexisting sites with no long-range order with the occurrence of an ordering transition, leading to the formation of the one-dimensional linear metallic chains observed at the monolayer coverage. The adsorbate-adsorbate interaction appears to be the leading driving force in this ordering transition which shows that it should be taken into account in theoretical calculations. Finally, the K atoms are bonded to the Si surface through the Si dangling bond, which suggests that cave would be favorable as the site of adsorption and agrees very well with the *ab initio* all-electron total-energy molecular theoretical calculations.<sup>8</sup> The proposed structural model of K adsorption on the Si(100)2×1 surface obtained on the basis of the present STM and synchrotron-radiation photoemission experiments are in excellent agreement with our recent study of the similar Na/Si(100)2×1 system using a very different experimental technique, namely photoemission EXAFS. This investigation brings new insights into the understanding of the structural properties of (alkali metal)/Si(100)2×1 systems.

## ACKNOWLEDGMENTS

This work was supported by the U.S. National Science Foundation under Grant No. DMR 88-07754 and by the Commissariat à l'Énergie Atomique (CEA). The technical staff of the Synchrotron Radiation Center at the University of Wisconsin-Madison is also acknowledged for helpful and expert technical assistance. One of us (P.S.) wishes to thank the Xerox Webster Research Center for its kind hospitality.



- \*Also at Department of Physics, Northern Illinois University, DeKalb, Illinois 60115-2854.
- <sup>1</sup>Physics and Chemistry of Alkali Metals Adsorption, edited by H. P. Bonzel, A. M. Bradshaw, and G. Ertl, Mater. Sci. Monographs 57 (Elsevier, Amsterdam, 1989), and references therein.
- <sup>2</sup>Metallization and Metal/Semiconductor Interfaces, Vol. 195 of NATO Advanced Study Institute, Series B: Physics, edited by I. P. Batra (Plenum, New York, 1989), and references therein.
- <sup>3</sup>P. Soukiassian, in *Fundamental Approach to New Materials Phases—Ordering at Surfaces and Interfaces*, edited by A. Yoshimori, T. Shinjo, and H. Watanabe, Springer Series in Materials Science Vol. 17 (Springer-Verlag, Berlin 1992), p. 197.
- <sup>4</sup>T. Aruga, H. Tochiwara, and Y. Murata, Phys. Rev. Lett. **53**, 372 (1984).
- <sup>5</sup>M. Tsukada, H. Ishida, and N. Shima, Phys. Rev. Lett. **53**, 376 (1984).
- <sup>6</sup>T. Kendelewicz, P. Soukiassian, R. S. List, J. C. Woicik, P. Pianetta, I. Lindau, and W. E. Spicer, Phys. Rev. B **37**, 7115 (1988).
- <sup>7</sup>P. Soukiassian, M. H. Bakshi, Z. Hurych, and T. M. Gentle, Surf. Sci. Lett. **221**, L759 (1989).
- <sup>8</sup>Ye Ling, A. J. Freeman, and B. Delley, Phys. Rev. B **39**, 10 144 (1989).
- <sup>9</sup>J. Levine, Surf. Sci. **34**, 90 (1973).
- <sup>10</sup>H. Tochiwara, Surf. Sci. **126**, 523 (1983).
- <sup>11</sup>Ye Ling and Xie Xide, Surf. Sci. Lett. **247**, L204 (1991).
- <sup>12</sup>C. M. Wei, H. Huang, S. Y. Tong, G. S. Glander, and M. B. Webb, Phys. Rev. B **42**, 11 284 (1990); G. S. Glander and M. B. Webb, Surf. Sci. **222**, 64 (1989).
- <sup>13</sup>S. T. Kim, P. Soukiassian, L. Barbier, S. Kapoor, and Z. Hurych, Phys. Rev. B **44**, 5622 (1991).
- <sup>14</sup>S. Nishigaki, S. Matsuda, T. Sasaki, N. Kawanishi, Y. Ikeda, and H. Takeda, Surf. Sci. **231**, 271 (1990); S. Nishigaki, S. Matsuda, T. Sasaki, N. Kawanishi, H. Takeda, and A. Kawase, Vacuum **41**, 632 (1990).
- <sup>15</sup>H. Ishida and K. Terakura, Phys. Rev. B **40**, 11 519 (1989).
- <sup>16</sup>M. Tikhov, G. Rangelov, and L. Surnev, Surf. Sci. **231**, 280 (1990).
- <sup>17</sup>T. Abukawa and S. Kono, Phys. Rev. B **37**, 9097 (1988); Surf. Sci. **214**, 141 (1989).
- <sup>18</sup>S. Kennou, S. Ladas, M. Kamaratos, and C. A. Papageorgopoulos, Surf. Sci. **216**, 462 (1989).
- <sup>19</sup>Y. Hasegawa, I. Kamiya, T. Hashizume, T. Sakurai, H. Tochiwara, M. Kubota, and Y. Murata, Phys. Rev. B **41**, 9688 (1990).
- <sup>20</sup>A. J. Smith, W. R. Graham, and E. W. Plummer, Surf. Sci. Lett. **243**, L37 (1991).
- <sup>21</sup>T. Urano, Y. Uchida, S. Hongo, and T. Kanaji, Surf. Sci. **242**, 39 (1991).
- <sup>22</sup>T. Makita, S. Kohmoto, and A. Ichimiya, Surf. Sci. **242**, 65 (1991).
- <sup>23</sup>G. R. Castro, P. Pervan, E. G. Michel, R. Miranda, and K. Wandelt, Vacuum **41**, 565 (1990).
- <sup>24</sup>I. P. Batra, Phys. Rev. B **39**, 3919 (1989).
- <sup>25</sup>Y. Morikawa, K. Kobayashi, K. Terakura, and S. Blügel, Phys. Rev. B **44**, 3459 (1991).
- <sup>26</sup>B. L. Zhang, C. T. Chan, and K. M. Ho, Phys. Rev. B **44**, 8210 (1991).
- <sup>27</sup>Preliminary accounts of this work have been reported by P. Soukiassian and J. A. Kubby, in *Structure of Surfaces — III*, edited by S. Y. Tong, X. Xide, K. Tagayanaki, and M. A. Van Hove, Springer Series in Surface Science Vol. 24 (Springer-Verlag, Berlin, 1991), p. 584; J. A. Kubby, W. J. Greene, and P. Soukiassian, J. Vac. Sci. Technol. B **9**, 739 (1991); and by P. Soukiassian, K. M. Schirm, P. S. Mangat, and Z. Hurych, Bull. Am. Phys. Soc. **37**, 224 (1992).
- <sup>28</sup>P. E. Wierenga, J. A. Kubby, and J. E. Griffith, Phys. Rev. Lett. **59**, 2169 (1987); J. E. Griffith, J. A. Kubby, P. E. Wierenga, R. S. Baker, and J. Vickers, J. Vac. Sci. Technol. A **6**, 493 (1988).
- <sup>29</sup>P. Soukiassian and H. I. Starnberg, in *Physics and Chemistry of Alkali Metals Adsorption* (Ref. 1), p. 449.
- <sup>30</sup>P. Soukiassian, R. Riwan, Y. Borenztein, and J. Lecante, J. Phys. C **17**, 1761 (1984).
- <sup>31</sup>P. Soukiassian, T. Kendelewicz, and Z. Hurych, Phys. Rev. B **40**, 12 570 (1989).
- <sup>32</sup>R. Riwan, P. Soukiassian, S. Zuber, and J. Cousty, Surf. Sci. **146**, 382 (1984).
- <sup>33</sup>P. Soukiassian, and R. Riwan (unpublished).
- <sup>34</sup>P. Soukiassian, R. Riwan, J. Lecante, E. Wimmer, S. R. Chubb, and A. J. Freeman, Phys. Rev. B **31**, 4911 (1985).
- <sup>35</sup>J. A. Kubby, Y. R. Wang, and W. J. Greene, Phys. Rev. Lett. **65**, 2165 (1990).
- <sup>36</sup>Y. Enta, T. Kinoshita, S. Suzuki, and S. Kono, Phys. Rev. B **36**, 9801 (1987).
- <sup>37</sup>P. Soukiassian, M. H. Bakshi, Z. Hurych, and T. M. Gentle, Phys. Rev. B **35**, 4176 (1987); H. I. Starnberg, P. Soukiassian, and Z. Hurych, *ibid.* **39**, 12 775 (1989); H. I. Starnberg, P. Soukiassian, M. H. Bakshi, and Z. Hurych, Surf. Sci. **224**, 13 (1989), and references therein.
- <sup>38</sup>Z. Hurych, H. I. Starnberg, and P. Soukiassian, Europhys. Lett. **8**, 567 (1989).
- <sup>39</sup>G. E. Rhead, Appl. Surf. Sci. **52**, 19 (1991).
- <sup>40</sup>P. Soukiassian, Surf. Sci. Lett. **172**, L 507 (1986).
- <sup>41</sup>P. Soukiassian and T. Kendelewicz, in *Metallization and Metal/Semiconductor Interfaces* (Ref. 2), p. 465.
- <sup>42</sup>Y. Ma, J. E. Rowe, E. E. Chaban, C. T. Chen, R. L. Headrick, G. M. Meigs, S. Modesti, and F. Sette, Phys. Rev. Lett. **65**, 2173 (1990).
- <sup>43</sup>L. S. O. Johansson and B. Reihl, Phys. Rev. Lett. **67**, 2191 (1991).
- <sup>44</sup>Ye Ling, A. J. Freeman, and B. Delley, Surf. Sci. Lett. **239**, L 526 (1990).
- <sup>45</sup>E. Wimmer, C. L. Fu, and A. J. Freeman, Phys. Rev. Lett. **55**, 2618 (1985).
- <sup>46</sup>B. Hellsing, Phys. Rev. B **40**, 3855 (1989).
- <sup>47</sup>Y. J. Chabal and K. Raghavachari, Phys. Rev. Lett. **53**, 282 (1984); **54**, 1055 (1985); J. E. Northrup, Phys. Rev. B **44**, 1419 (1991).
- <sup>48</sup>P. S. Mangat, P. Soukiassian, K. M. Schirm, and Z. Hurych (unpublished).

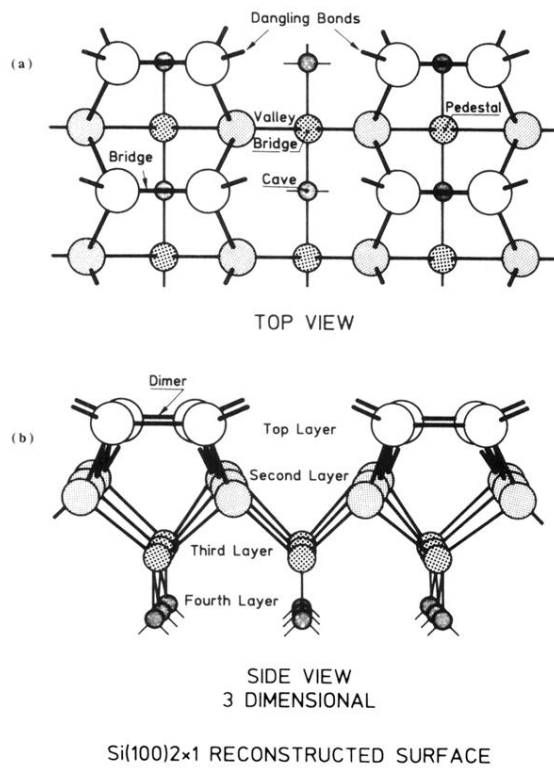


FIG. 1. Top view model of the reconstructed Si(100)2×1 surface showing the various possible adsorption sites for K atoms proposed in the literature. (b) Three-dimensional 3(D) side view model of the reconstructed Si(100)2×1 in the case of symmetric dimers.

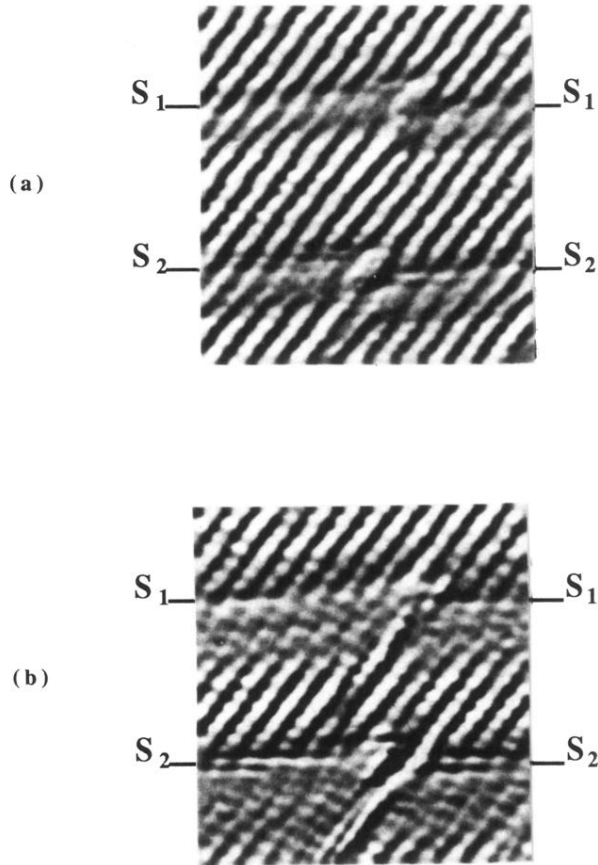


FIG. 3. Curvature STM image (filled states) of 1 ML of potassium on the Si(100) $2\times 1$  ( $4^\circ$ )-stepped surface. The tip bias was  $V_t = +1.2$  V and the tunneling current was 1 nA. The two steps are noted as  $S_1$  and  $S_2$ . The potassium chains are formed along the  $\langle 110 \rangle$  direction and the distance between two chains is 7.68 Å. Notice the two 3D potassium clusters on the step edges. The image has not been corrected for drift. The maximum pressure rise  $\Delta P$  during potassium deposition remained below  $1\times 10^{-11}$  Torr. (b) Curvature STM image (empty states) of 1 ML of potassium on the Si(100) $2\times 1$ ( $4^\circ$ )-stepped surface. The tip bias was  $V_t = -1.2$  V and the tunneling current was 1 nA. The two steps are noted as  $S_1$  and  $S_2$ . The maximum pressure rise  $\Delta P$  during potassium deposition remained below  $1\times 10^{-11}$  Torr.

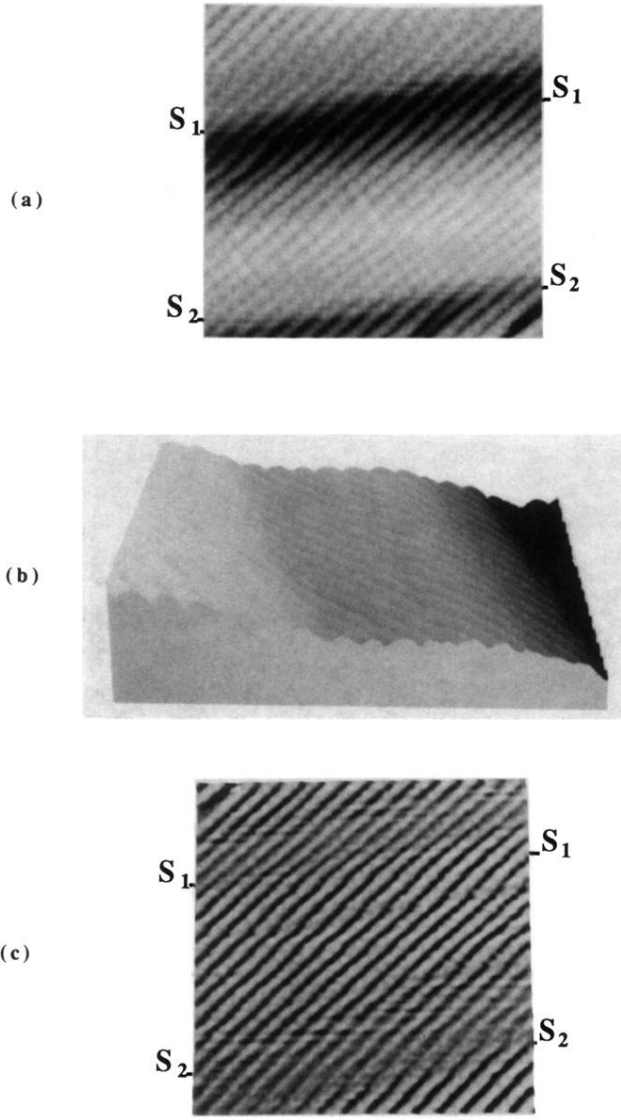


FIG. 4. (a) Height STM image (filled states) of 1 ML of potassium on the Si(100) $2\times 1$  for another area. The two steps are noted as  $S_1$  and  $S_2$ . The image has not been corrected for drift. The tip bias was  $V_t = +1.2$  V and the tunneling current was 1 nA. The maximum pressure rise  $\partial P$  during potassium deposition remained below  $1 \times 10^{-11}$  Torr. (b) 3D side view of (a). (c) Curvature map of (a). The two steps are noted as  $S_1$  and  $S_2$ .

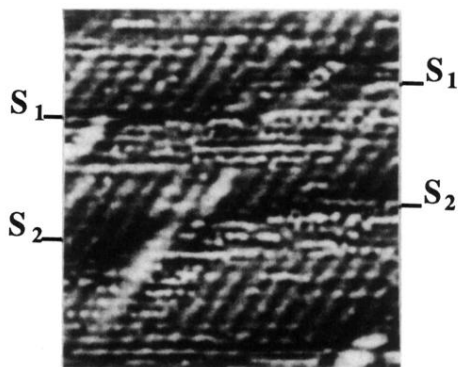


FIG. 5. Curvature STM image (filled states) of 0.4 ML of potassium on the Si(100) $2 \times 1$ - $4^{\circ}$ -stepped surface. The tip bias was  $V_t = +1.2$  V and the tunneling current was 1 nA. The two steps are noted as  $S_1$  and  $S_2$ . The image has not been corrected for drift. The maximum pressure rise  $\Delta P$  during potassium deposition remained below  $1 \times 10^{-11}$  Torr.